Supplemental Data: Cysteine reactivity and thiol-disulfide interchange pathways in AhpF and AhpC of the bacterial alkyl hydroperoxide reductase

Thomas J. Jönsson, Holly R. Ellis and Leslie B. Poole

Department of Biochemistry, Wake Forest University School of Medicine

Winston-Salem, North Carolina 27157

METHODS

Spectral and Anaerobic Measurements. All absorbance spectra and anaerobic titrations employed the thermostatted Milton Roy Spectronic 3000 diode array spectrophotometer. The oxidoreductase and DTNB assays were performed on a thermostatted Applied Photophysics DX.17MV stopped-flow spectrofluorometer. The molar extinction coefficients of the protein-bound FAD at 448 or 449 nm were determined by release of the flavin cofactor with 4.0 M guanidine hydrochloride and quantitation of the corresponding free FAD (*2*).

Anaerobic titrations were carried out essentially as previously described (*3*). NADH titrating solutions were prepared in buffer bubbled for 20-30 min with oxygen-free nitrogen, loaded into the titrating syringe, and standardized prior to each experiment. An oxygen-scrubbing system consisting of protocatechuate 3,4-dioxygenase and protocatechuic acid was included in all NADH titration experiments. Spectral data were not corrected for dilution, which was <3% overall.

Transhydrogenase and oxidase assays. Tranhydrogenase assays were carried out at 25°C in 1 mL of solution containing 150 μM each of NADH and $AcPyAD^+$, 50 mM Tris-HCl at pH 8.0, 0.5 mM EDTA, 100 mM ammonium sulfate, and 10-20 pmol of AhpF monitoring the gain in absorbance at 390 nm due to the formation of AcPyADH (*2*).

Oxidase assays were performed at 25 °C in 1 mL of air-saturated buffer containing 150 μM NADH, 50 mM potassium phosphate at pH 7.5, 0.5 mM EDTA, and 30-60 pmol of AhpF, monitoring absorbance changes at 340 nm.

Identification of the interdomain disulfide-containing peptide. Ten nmol of the interdomain disulfide-bonded C132S/C345S mutant (species D, after DTNB treatment, Fig. 3B) containing the buried non-catalytic cysteines Cys476 and Cys489 was denatured in 6 M urea, 100 mM MES, pH 6.0, in the presence of 200-fold excess of 4-vinylpyridine (2.6 μL) at room temperature to prevent scrambling of thiol disulfide bonds (*3*). The 4-vinylpyridine was removed by extensive dialysis in a 10 kDa cut off Slide-a-Lyzer (Pierce) against 5 L of 5 mM MES, pH 6.0, and then 5 L of deionized H_20. The labeled protein was resuspended in 8 M urea solution. Dilutions were made to reach 2 M urea and 100 mM Tris-HCl at pH 8.0 in a final volume of 500 μL, and the samples were incubated overnight at 37°C after the addition of 5.7 μg TPKC-treated trypsin (1/100 w/w). Approximately 10 μg of protein was injected onto a reverse phase C4 column (Vydac) connected to a VG Quattro II triple quadrupole mass spectrometer. The peptides were eluted using a gradient of 0 to 70% acetonitrile (in 0.1% TFA) over 65 minutes. The purification of the interdomain disulfide-containing peptides was performed on a Waters analytical HPLC system using a reverse phase C4 column (Vydac). Peaks were detected at 215 nm. The isolated peptide was reduced by DTT and injected onto the C4 column connected to the mass spectrometer.

Limited tryptic digestions. Reduced and DTNB-oxidized forms of C132S/C345S AhpF were digested in two different buffer solutions; buffer A consisted of 50 mM Tris-HCl at pH 8.0, 0.5 mM EDTA, 100 mM ammonium sulfate and buffer B consisted of 25 mM potassium phosphate at pH 7.0, 1 mM EDTA. One μg of TPCK-treated trypsin (1/100 w/w) was added to C132S/C345S and aliquots were removed after 5, 10 and 30 minutes and quenched by heating to 70°C for 3 min in 0.5 % SDS and 10 mM N-ethylmaleimide, then maintaining the samples on ice. Ten μg was loaded in each lane on reducing SDS polyacrylamide gels.

Reactivity of AhpC mutants with TNB-linked AhpF mutants. The respective single cysteine mutants of AhpC (115-300 μM) were added to 15 μM of the indicated TNB-linked AhpF mutant in 25 mM potassium phosphate 1mM EDTA pH 7.0 at 25°C. The release of TNB was observed at 412 nm and fit to a first order rate equation. The second order rate constant was then calculated.

Anaerobic fluorescence NADH titration. Ten to fifteen μM solution of wild type AhpF, C132S AhpF, TNB-linked C132S AhpF, or complexed F:Cys129-S-S-Cys165:C were prepared in buffer made anaerobic by repeated evacuation and argon flushing of the solutions for 20-30 min. Excitation was set for 340 nm and the emission was collected at 410 nm until no change in fluorescence was observed (~20 min) after each addition of NADH. The fluorescence emission data were not corrected for dilution, which was <3% overall.

Analytical Ultracentrifugation Studies. Sedimentation velocity studies were conducted at 20 ˚C in standard 12 mm path-length, double-sectored cells (using an Optima XL-A analytical ultracentrifuge, Beckman Instruments, Palo Alto, CA) and data were analyzed using SVEDBERG (version 6.39) software (www.jphilo.mailway.com) as described previously (*4*). A value of 0.73929 cm^3/g was calculated for the partial specific volume of disulfide-linked C46S AhpC and C132S mutant of the AhpF N-terminal domain based on the amino acid composition (*5*).

RESULTS

Spectral characteristics of single cysteine mutants of AhpF. Each of the redox-active cysteine residues of AhpF was individually substituted by a serine residue (at C129, C132, C345 and C348); an additional AhpF mutant lacking all four catalytic cysteine residues was also constructed (4C→S). Comparisons of the visible absorbance spectra of C129S, C132S, C345S and 4C→S mutant AhpF proteins showed nearly identical spectral properties for these mutants when compared with the wild type enzyme (Table S1). Only the C348S mutant showed altered spectral properties, with maxima at 373 and 445 nm (relative to 377-381 nm and 448-449 nm for

Table S1. Spectral properties of the the wild type and single cysteine mutant AhpF proteins.

	wild type[a]	C129S	C132S	C345S[b]	C348S[b]	4C→S
Molar extinction coefficient[c]	13,000 ± 700	13,200 ± 100	13,600 ± 200	12,500 ± 900	12,300 ± 800	12,600 ± 200
λ_{max} of two flavin peaks (nm)	381, 449	380, 448	380, 448	381, 449	373, 445	377, 449
Ratio of absorbances[d]	1.04	1.03	1.03	1.00	1.20	1.10

[a] Ref. (*1*)
[b] Molar extinction coefficents, λ_{max} of two flavin peaks, and ratio of absorbances were reported in ref *18*.
[c] Results are from 445,448 or 449 nm, and are shown as mean ± standard deviation (two to four relicates) expressed as M^{-1} cm^{-1}.
[d] The ratio is the absorbance of the flavin peak around 448 nm range divided by that of the flavin peak around 380 nm.

the other mutants and wild type AhpF) and a significantly lower extinction coefficient for the 373 nm peak.

*Spectral Analyses of AhpF Double Cysteine Mutant*s. Comparisons of the visible absorbance spectra of the two AhpF mutants C132S/C345S and C129S/C345S, in standard phosphate buffer (summarized in Table S2), indicated similar spectral properties for these mutants with those of wild type AhpF. The flavin fluorescence properties of these two mutants are similar to that of wild type enzyme. The two other active site mutants, C132S/C348S and C129S/C348S, showed significant differences in having a blue-shifted flavin peaks at 374 nm with a significantly lower extinction coefficient. This is consistent with the spectral characteristics of the above mentioned one cysteine mutant C348S. In addition, a decrease in fluorescence of 18 and 40% for C132S/C348S5 and C129S/C348S, respectively, was observed.

Retention of Transhydrogenase and Oxidase Activities by AhpF Double Cys Mutants. Flavin-mediated transhydrogenase and oxidase assays were performed to ascertain the proper functionality of the bound flavin in the AhpF mutants. Whereas transhydrogenase activity assesses hydride transfer from NADH to a pyridine nucleotide analogue of higher potential ($AcPyAD^+$) by the enzyme's bound flavin, the oxidase activity arises from the transfer of a pair of electrons from NADH to O_2. Previous active site mutant studies of AhpF have indicated that Cys345 in the absence of Cys348 promotes a higher transhydrogenase activity (*1*), although this

Table S2. Spectral properties of the the wild type and double cysteine mutant AhpF proteins.

Protein	AhpF (wt)[a]	C132S/C348S	C132S/C345S	C129S/C348S	C129S/C345S
Molar extinction coefficient [b]	13,000 ± 660	12,020 ± 200	11,360 ± 120	11,050 ± 120	11,200 ± 250
λ_{max} of two peaks	381, 449	374, 447	382, 449	374, 447	382, 449
Ratio of flavin peak absorbance [c]	1.04	1.12	1.02	1.18	0.97
Fluorescence [d]	1.00	0.82	1.11	0.60	1.09
Oxidase activity [e]	108 ± 4	211 ± 19	284 ± 51	231 ± 25	251 ± 35
Transhydrogenase activity [f]	2730 ± 140	1700 ± 70	1870 ± 130	1550 ± 70	1870 ± 100

[a] Ref. (*1*) [b] Results for C132S/C348S and C129S/C348S are for 447 nm or, in the case of C132S/C345S and C129S/C345S, for 449 nm, and are shown as mean ± standard error (three replicates) expressed as M^{-1} cm^{-1}. [c] The ratio is of the absorbance of the flavin peak at 447/449 nm divided by that of the flavin peak at 374/382 nm. [d] Fluorescence intensity is shown relative to wild-type AhpF at 1.0, a value which is 24% that of an equivalent concentration of free FAD. Activity results reported as mean ± standard error are expressed as micromoles of substrate reduced per minute relative to micromoles of FAD determined at 450 nm. [e] Results were obtained for 30 and 60 pmol of each protein. [f] Results were obtained using 10-20 pmol of each protein.

was not observed in either of the double active site cysteine mutants retaining Cys345 (C129S/C348S and C132S/C348S). All oxidase activities of the double mutants were about 2 to 2.6-fold higher than that of AhpF. Thus, as summarized in Table S2, the oxidase and transhydrogenase activities are fully retained and independent of the thiol status in the active sites. These mutants were therefore appropriately folded as measured by flavin-mediated enzymatic activity.

Stabilization of a Charge Transfer Absorbing Species in Double Cysteine Mutants of AhpF. A charge-transfer interaction between the thiolate of C348 and FAD was observed in amine-containing buffers including both Tris and ammonium sulfate for the single mutant and two double mutants of AhpF containing the C345S mutation. The strongest interaction is observed for the C132S/C345S mutant. This charge transfer absorbance band was weaker in ammonium sulfate or Tris buffer alone; their combination, however, showed a synergistic effect in enhancing the charge transfer absorbance band, giving a maximum extinction coefficient at 530 nm of 4400 M^{-1} cm^{-1} (Fig. 2B). The removal of the amine-containing buffers by dialysis resulted in the disappearance of the charge transfer band, whereas an increase in conductivity by

NaCl or KCl did not affect the charge transfer band. Interestingly, protonation of C348 by lowering the pH decreased the thiolate-FAD charge transfer band at pH ≤7.5, with a complete absence at pH 5.5.

Confirmation of intercenter disulfide bond in oxidized C132S/C345S by tryptic digests and mass spectrometry. The thiol quantitation of DTNB-treated C132S/C345S suggested that a disulfide bond had been formed. To confirm that the proper intramolecular disulfide bond had been formed, DTNB-treated C132S/C345S was digested under denaturing conditions and resolved on a reverse column attached to an electrospray ionization triple quadrupole mass spectrometer (ESI-MS). In comparing the chromatogram (Fig. S1) of the disulfide-containing peptide mixture with that of the DTT-treated mixture, a strong peak observed in the oxidized sample at 45 min was lost upon treatment with DTT. The mass of this species, PepAB, at 5492.1 amu corresponds to the expected disulfide-bonded active site peptides (PepA and PepB predicted at 5491.5 amu). In the reduced sample we were unable to find the two individual peptides PepA

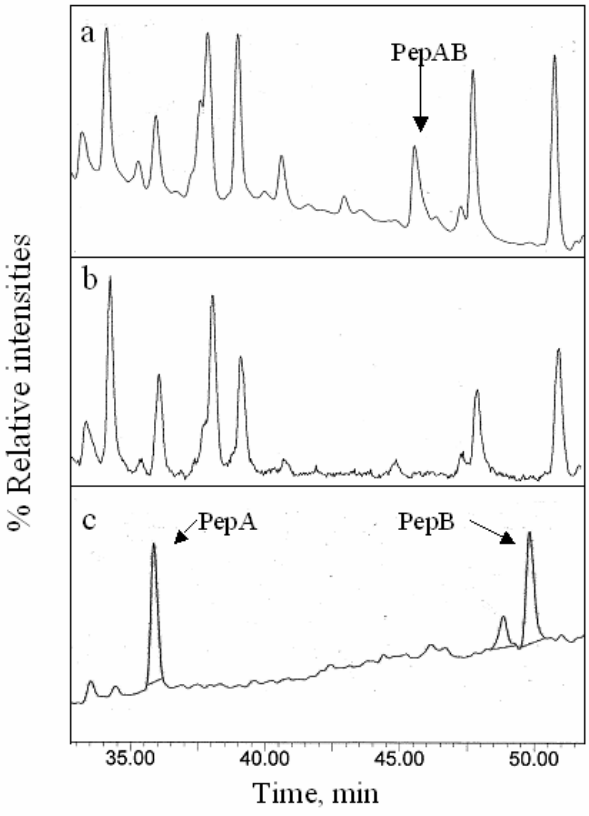

Figure S1. HPLC-ESI-MS identification of tryptic peptides from the DTNB-oxidized C132S/C348S mutant of AhpF. For molecular analyses of peptides, exhaustive digestion of the DTNB-oxidized C132S/C348S mutant of AhpF was carried out, followed by fractionation on a Vydac C4 column and diversion of a small part of that eluate to a triple quadrupole mass spectrometer. Panels A and B show the absorbances at 215 nm of the eluates from the column of the digest either without (A) or with (B) pretreatment of the sample with DTT. Following isolation of "PepAB" eluting at 45 min in panel A (5492.1 amu), DTT was added and the sample was reanalyzed by chromatography and mass spectrometry (panel C, with total ion current plotted rather than absorbance). The two major peaks, PepA and PepB, eluted at 36 and 50 min, and had masses of 1520 and 3973 amu, respectively. Sequences of the corresponding peptides are GVTYSPHCDGPLFK (PepA) and DIDGDFEFETYYSLSCHNSPDVVQALNLMA VLNPR (PepB).

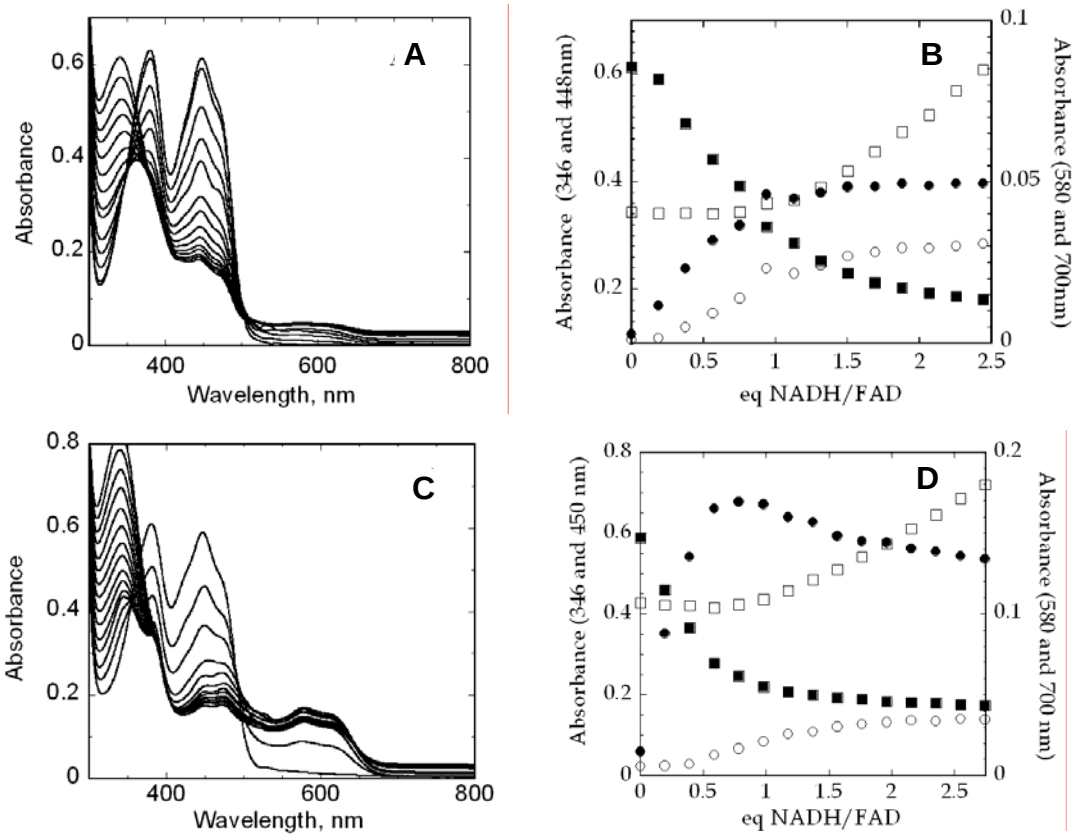

Figure S2. Anaerobic NADH titration of oxidized and reduced forms of AhpF mutant C132S/C345S. The dithiol form (26 nmol, panels A and B) and interdomain disulfide-bonded form (24 nmol, panel C and D) in standard phosphate buffer at neutral pH was titrated with a 3.8 mM anaerobic solution of NADH. Solid lines in *panel A* represent spectra obtained after the addition of multiple aliquots of 0.19 equiv each of NADH/FAD (A_{448} decreasing and A_{580} increasing); similarly, spectra shown in panel C were taken after the addition of multiple aliquots of 0.20 equiv each of NADH/FAD. Spectra (panels A and C) were recorded after each addition when no further absorbance changes occurred. Panels B and D show the absorbance changes at 346 (open squares), 448 or 450 (closed squares), 580 (closed circles), and 700 nm (open circles) *versus* equiv of NADH/FAD added.

and PepB. Thus a large amount of PepAB was purified separately and then injected onto a reverse column attached to the ESI-MS (Fig. S1). This resulted in the identification of the two peptides, PepA eluting at 36 min (1520 amu) and PepB eluting at 50 min (3973 amu), corresponding to their predicted masses. Thus the DTNB treatment of C132S/C345S results in the formation of a disulfide bond between C348 in the C-terminal region and C129 in the N-terminal domain.

Reductive NADH titration of oxidized and reduced C132S/C345S. As shown in Figure S2, anaerobic titration of recombinant AhpF with NADH leads to the gradual loss of 450 nm absorbance. In both conformations of C132S/C345S the oxidation of NADH, monitored at 350

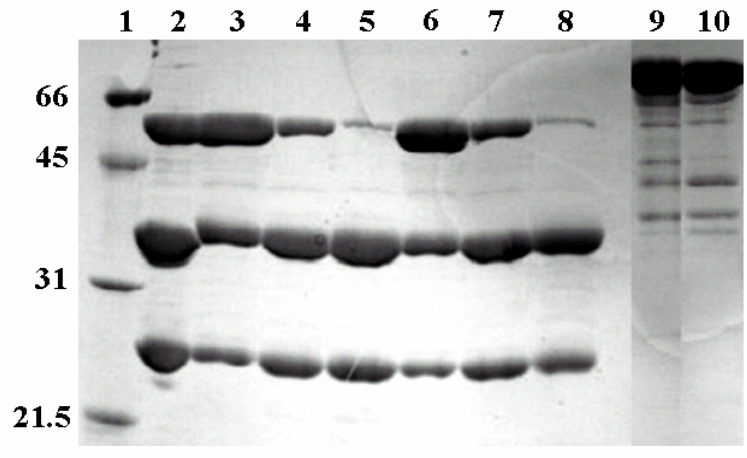

Figure S3. Limited tryptic digest of the interdomain disulfide bond-containing and dithiol forms of AhpF mutant C132S/C345S. From left, lane 1, Broad Range Molecular Weight Standards (Bio-Rad); lane 2, Recombinant purified proteins wild type AhpF 57kDa, C-terminal fragment (F[208-521], 35 kDa) and N-terminal domain (F[1-202], 22 kDa); lanes 3-5, 3 min, 10 min and 30 min time course of trypsin-treated dithiol form of C132S/C345S in 25 mM potassium phosphate pH 7.0; lanes 6-8, 3 min, 10 min and 30 min time course of trypsin-treated dithiol form of C132S/C345S in 50 mM Tris, 100 mM ammonium sulfate at pH 8.0; lane 9, 30 minute tryptic digest of interdomain disulfide bond-containing C132S/C345S in 25 mM potassium phosphate pH 7.0; lane 10, 30 minute tryptic digest of interdomain disulfide bond-containing C132S/C345S in 50 mM Tris, 100 mM ammonium sulfate at pH 8.0.

nm where the conversion of oxidized flavin to semiquinone is isosbestic and by the breakpoint in the decrease in 450 nm absorbance, account for approximately 0.7 to 0.9 equiv/FAD. This suggests that the disulfide bond in the oxidized C132S/C345S is inaccessible to reduction by FAD. No difference between the dithiol and disulfide bonded forms was seen in the $FADH_2 \rightarrow NAD^+$ charge-transfer band at 700 nm. In the dithiol form of C132S/C345S, the extent of formation of stable semiquinone ($FADH^{\bullet}$) is similar to that of wild-type AhpF. The extent of semiquinone formation is roughly 65%. However, in the disulfide-bonded C132S/C345S, only 20% of the total flavin is in the semiquinone form at the end of the titration and the consumption of NADH is closer to 1 equiv/FAD. A 10% increase in fluorescence in the oxidized form compared to the dithiol was observed. The significant difference in semiquinone formation suggests that the flavin environment is different in the two species.

Limited tryptic digest. The two conformations represented by the dithiol and oxidized form of C132S/C345S would be expected to have different susceptibility to proteolysis due to differences in surface accessible residues. AhpF consists of two modules, F[1-202] and F[208-

Table S3. Reactivity of AhpC mutants with TNB-linked AhpF mutants[a].

	TNB-linked C132S AhpF	TNB-linked C129S AhpF
C165S AhpC	1270 ± 93	26.9 ± 2.4
C46S AhpC	1460 ± 140	67.2 ± 2.9

[a] The respective cysteine mutant of AhpC (115-300 μM) was added to 15 μM of the indicated TNB-linked AhpF in 25 mM potassium phosphate, 1 mM EDTA, pH 7.0 at 25 °C. The release of TNB was observed at 412 nm and fit to a first order rate equation. The second order rate constant was then calculated. Values are expressed as M^{-1} s^{-1}.

521], that are connected by a short linker region (*6, 7*). Previous limited tryptic digest of AhpF isolated a stable 37 kDa fragment but not the F[1-202] domain (*3*). This suggests that the F[1-202] region is very mobile and the linker region is very accessible to trypsin. Limited tryptic digest of the dithiol and oxidized forms of C132S/C345S in a Tris/ammonium-containing buffer, where we can observe the thiolate → FAD charge transfer, and our standard phosphate buffer showed that the dithiol form is rapidly digested into two stable domains (Fig. S3). These two domains are consistent with the sizes of the two previously-studied fragments of AhpF, F[1-202] and F[208-521] (Fig S3, lane 2). In contrast, the interdomain disulfide bonded species was very protease resistant. After 30 min the oxidized form was >90% intact, suggesting that F[1-202] is packed closely to F[208-521], which would make the linker region less accessible. No difference was observed between the two buffer conditions.

Formation of covalent complexes between AhpF and AhpC mutants. As described in the main text, complex formation between reduced AhpF and TNB-linked conjugates of C46S or C165S AhpC showed high specificity; only reaction between C132S AhpF and TNB-linked C46S AhpC was efficient. As dithiol-disulfide exchange is generally a reversible reaction, the "reverse" experiments were also conducted; mixed disulfide adducts of TNB with AhpF mutants C129S and C132S were incubated with excess amounts of each AhpC mutant. Both C165S and C46S mutants of AhpC were able to attack both AhpF mutant TNB-linked disulfide bonds (Table S3), supporting the previous observation that both AhpC Cys residues can be sufficiently accessible and reactive for attack on disulfide bonds such as the one in DTNB (*8*). The AhpC

attack on TNB-linked C129 of AhpF, similar whether C46S or C165S was used, was at least 20-fold faster than on TNB-linked C132 (Table S3). Note, however, that the observed rate of disulfide bond formation of 1460 M^{-1} s^{-1} for the attack of AhpC on an AhpF disulfide bond was three orders of magnitude slower than that observed for the forward reaction between AhpF C132S and AhpC C46S-TNB. This suggests that the forward reaction is favored kinetically in addition to the likely thermodynamic preference for AhpC reduction by AhpF.

Electrospray Ionization Mass Spectrometry Analysis of the High Molecular Weight Complexes Formed Between AhpF and AhpC Mutants. After incubating TNB conjugates of either C46S or C165S AhpC with C132S AhpF, only three species were observed in each sample, one for the TNB conjugate present, one for C132S AhpF, and a higher molecular weight species with masses of 76,533 ± 1.3 and 76,542 ± 7.1 amu, respectively, for the samples generated with C46S or C165S AhpC. The expected mass for a simple 1:1 disulfide complex between the AhpF and AhpC mutants would be 76,528 amu (AhpC mutants, 20,600 amu each; C132S mutant of AhpF, 55,930 amu without FAD). This result strongly supports the identification of the major higher molecular weight complex observed on the SDS-polyacrylamide gel as an AhpF-AhpC complex containing an interprotein disulfide bond.

Anaerobic NADH titrations of C132S AhpF constructs and the F:C129-S-S-C165:C complex. As shown previously, NADH titration of wild type AhpF consumed 2.5 equivalents of NADH (*3*). Disruption of the N-terminal disulfide center in AhpF C132S resulted in the consumption of only 1.5 equivalents of NADH during similar titrations (Fig. S4). However, the formation of a mixed TNB disulfide in the AhpF mutant C132S prior to titrations, regenerating a reducible disulfide at the N-terminus of AhpF, established that there is redox communication between the intact C345-C348 disulfide bond and the N-terminus in this construct. In contrast, the purified protein complex AhpF:C129-S-S-C165:AhpC, when titrated anaerobically with NADH, indicated that approximately 1.5 equivalents of NADH per subunit were oxidized during the titration. Thus, TNB disulfide bonded to AhpF:C129 was small enough to allow electron transfer from the C-terminal disulfide center of AhpF. However, the conjugation of AhpF with

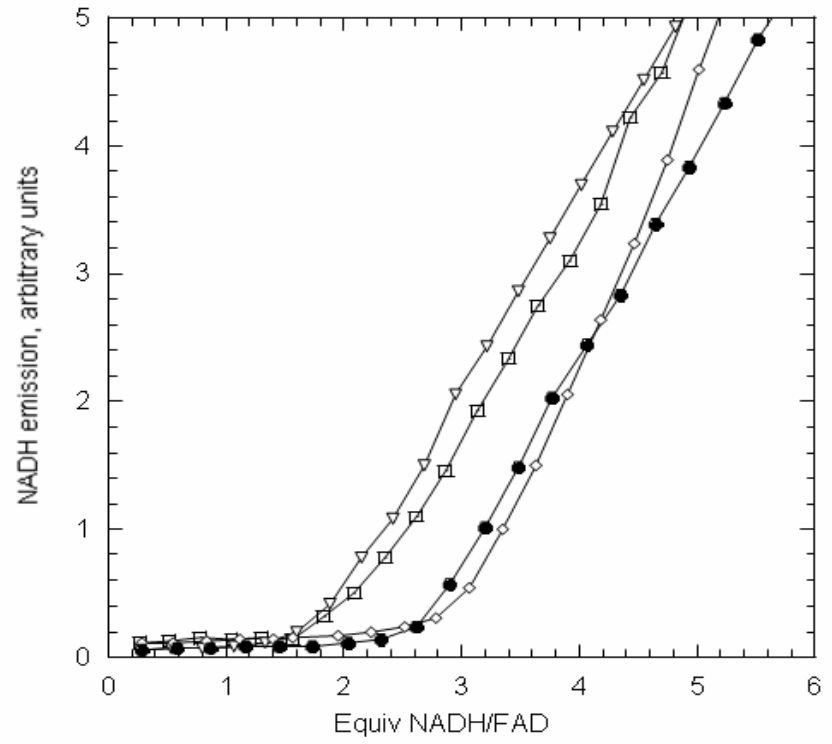

Figure S4. Anaerobic NADH titration of various AhpF and AhpC containing species monitored by fluorescence of NADH. Wild–type AhpF (closed circles), TNB conjugated AhpF Cys132Ser (open diamonds), AhpF Cys132Ser (open triangles) and engineered complex between AhpF and AhpC (F:Cys129-S-S-Cys165:C, open squares) at ~15 μM were titrated anaerobically with an anaerobic solution of 1.5-2.0 mM NADH. The samples were excited at 340 nm and fluorescence emissions were recorded at 460 nm.

AhpC produced a product that was too large a substrate for intramolecular interaction with the C-terminal disulfide bond of AhpF.

Biophysical Analyses of F:C129-S-S-C165:C. Previous studies have indicated that the crystal structures of oxidized and reduced AhpC are toroid-shaped decamers (*4, 9*). Based on analytical ultracentrifugation studies, reduced AhpC behaves as a concentration-independent decamer in solution, whereas oxidized AhpC is a dimer at low concentration (2.5 μM) and a decamer at high concentration (453 μM) (*4*). In order to assess the oligomeric nature of the F:C129-S-S-C165:C complex, sedimentation velocity ultracentrifugation analyses were performed. A heterogeneous distribution of complex species was observed. The predominant species had a sedimentation coefficient of 15 S and a second less prevalent species had a value of 6.8 S [compared with sedimentation coefficients of 6.7 and 8.7 for oxidized and reduced

decamers of AhpC, respectively (*4*)]. This heterogeneous behavior may be due to weakening of the decamer interface in AhpC by the attachment of AhpF, and/or the ability of AhpF, as a dimer, to crosslink AhpC on different dimers or decamers. To better understand the extent to which disulfide bond formation between AhpF and C165 of AhpC affects the decameric structure of AhpC without involving the complicating dimeric nature of AhpF, the separately-expressed, monomeric N-terminal fragment (residues 1-202) of AhpF (*6*) containing the C132S mutation was used to generate the disulfide-linked complex with the C46S mutant of AhpC using the corresponding DTNB conjugation procedure. At the lowest concentration evaluated, ~3.3 μM of covalently linked subunits, sedimentation velocity experiments indicated the presence of an apparently homogeneous 10.8 S species that, together with the diffusion coefficient (D = 1.68 F), yielded a calculated molecular weight of about 629,000 g/mol, a little larger than the total molecular weight expected for 10 subunits of each protein assembled according to the decameric AhpC scaffold (428,920 g/mol), but potentially reflecting the fully assembled complex. With higher concentrations of 9 and 15 μM, the complex mixtures observed precluded such analyses.

REFERENCES

1. Li Calzi, M., and Poole, L. B. (1997) Requirement for the two AhpF cystine disulfide centers in catalysis of peroxide reduction by alkyl hydroperoxide reductase, *Biochemistry 36*, 13357-13364.
2. Poole, L. B., and Ellis, H. R. (1996) Flavin-dependent alkyl hydroperoxide reductase from *Salmonella typhimurium*. 1. Purification and enzymatic activities of overexpressed AhpF and AhpC proteins, *Biochemistry 35*, 56-64.
3. Poole, L. B. (1996) Flavin-dependent alkyl hydroperoxide reductase from *Salmonella typhimurium*. 2. Cystine disulfides involved in catalysis of peroxide reduction, *Biochemistry 35*, 65-75.

4. Wood, Z. A., Poole, L. B., Hantgan, R. R., and Karplus, P. A. (2002) Dimers to doughnuts: redox-sensitive oligomerization of 2-cysteine peroxiredoxins, *Biochemistry 41*, 5493-5504.

5. Laue, T. M., Shah, B. D., Ridgeway, T. M., and Pelletier, S. L. (1992) Computer-aided interpretation of analytical sedimentation data for proteins, in *Analytical ultracentrifugation in biochemistry and polymer science* (Harding, S. E., Rowe, A. J., and Horton, J. C., Eds.) pp 90-125, The Royal Society of Chemistry, Cambridge.

6. Poole, L. B., Godzik, A., Nayeem, A., and Schmitt, J. D. (2000) AhpF can be dissected into two functional units: tandem repeats of two thioredoxin-like folds in the N-terminus mediate electron transfer from the thioredoxin reductase-like C-terminus to AhpC, *Biochemistry 39*, 6602-6615.

7. Wood, Z. A., Poole, L. B., and Karplus, P. A. (2001) Structure of intact AhpF reveals a mirrored thioredoxin-like active site and implies large domain rotations during catalysis, *Biochemistry 40*, 3900-3911.

8. Ellis, H. R., and Poole, L. B. (1997) Roles for the two cysteine residues of AhpC in catalysis of peroxide reduction by alkyl hydroperoxide reductase from *Salmonella typhimurium*, *Biochemistry 36*, 13349-13356.

9. Wood, Z. A., Poole, L. B., and Karplus, P. A. (2003) Peroxiredoxin evolution and the regulation of hydrogen peroxide signaling, *Science 300*, 650-653.